Int. J. Electrochem. Sci., 9 **(2014)** 2101 - 2112

International Journal of
ELECTROCHEMICAL
SCIENCE
www.electrochemsci.org

Effect of Temperature on the Corrosion Behavior of Carbon Steel in Hydrogen Sulphide Environments

Yameng Qi[1], *Hongyun Luo*[1,*], *Shuqi Zheng*[2], *Changfeng Chen*[2], *Zhenguo Lv*[2], *Maoxian Xiong*[2]

[1] Key laboratory of Aerospace advanced materials and performance (Ministry of Education), School of Materials Science and Engineering, Beijing University of Aeronautics and Astronautics, Beijing 100191, P R China
[2] Department of Materials Science and Engineering, China University of Petroleum Beijing, Beijing 102249, P R China
[*]E-mail: luo7128@163.com

Received: 21 November 2013 / *Accepted:* 29 December 2013 / *Published:* 2 February 2014

The corrosion behavior of carbon steel exposed to hydrogen sulphide environment at different temperatures was investigated using the methods of weight-loss tests, electrochemical measurements, scanning electron microscopy (SEM) and X-ray diffraction (XRD). The results show that corrosion rate increased first and then decreased significantly with increasing temperature. As temperature increased, more fine and compact corrosion film was formed and the corrosion film converted from mackinawite to mackinawite/cubic FeS, indicating better protection to the steel. In addition, the solution equilibrium chemistry of dissolved H_2S at different temperatures was also calculated and analyzed. Compared to the decrease of H^+ concentration, corrosion films could play a more dominant role in the decrease in corrosion rate. Finally, a probable mechanism is proposed to interpret the reason for corrosion rate result of carbon steel at different temperatures based on the protectiveness of corrosion film and the variation of H^+ concentration.

Keywords: Carbon steel; Corrosion rate; Electrochemical impedance spectroscopy; Hydrogen sulphide environment; Temperature

1. INTRODUCTION

In recent years, more and more oil and gas fields containing hydrogen sulphide has been actively developed for the world-wide energy demand [1]. As a result, a great quantity of pipelines and oilfield equipment are required for the operation of oil and gas fields. However, when exposed to hydrogen sulphide environments, the applications of pipelines and oilfield equipment could be limited due to the sulphide stress corrosion cracking (SSCC), hydrogen-induced cracking (HIC) and hydrogen

sulphide (H_2S) corrosion. Many researches have focused on SSCC and HIC [2-8]. Furthermore, some related mechanisms have been proposed so far, such as hydrogen pressure theory (HP) [9], hydrogen induced weakness of the metallic lattice or hydrogen induced decohesion (HID) [10,11], hydrogen enhanced local plasticity (HELP) [12-14], etc. However, the H_2S corrosion has not been yet investigated systematically.

During the past 20 years, several previous studies have been performed related to the corrosion behavior of iron and steel in H_2S solutions [15-20]. In the literature, there are studies of the effect of H_2S on iron [15,16], carbon steel [17], steel weld [18] and heat-affected zone [19], the effect of H_2S concentration on steel [20]. These results showed that H_2S could accelerate both the anodic iron dissolution and the cathodic hydrogen evolution in most cases, but H_2S can also have a strong inhibition on the iron corrosion in certain special conditions with low H_2S concentration (below 0.04 mmol/dm^3), appropriate pH value (within 3-5) and long immersion time (over 2 h) [16]. However, these works investigated the effect of H_2S on the corrosion behavior at ambient temperature. Though some papers about H_2S corrosion have been carried out at 90 °C [21,22], the corresponding researches focused on the corrosion behavior of steel under a single temperature. Thus, the influence of temperature on the corrosion behavior of steel in hydrogen sulphide environments has not been yet investigated systematically.

Starting from the aforementioned insights, an experimental study was launched with the objective of researching the corrosion behavior of carbon steel exposure to hydrogen sulphide environment at different temperatures.

2. EXPERIMENTAL METHOD

2.1 Material and specimen preparation

The material under investigation was a flange forgings of A350LF2 steel with a chemical composition (wt.%): C 0.19, Si 0.18, Mn 0.81, S 0.021, P 0.029, Cr 0.10, Ni 0.033, Cu 0.026, Mo 0.006, V 0.002, and Fe balance. Specimens were cut into 50 × 10 × 3 mm for weight-loss tests, and 10 × 10 × 3 mm for corrosion film analysis. For the electrochemical measurement, the specimens were machined to a disc with 8 mm in thickness and 12 mm in outer diameter. Prior to the experiments, all specimens were ground sequentially on 320, 600, and 1000 grit carbide silicon paper, and then degreased with acetone, cleansed with distilled water and dried in air.

2.2 Corrosion tests

Corrosion tests were conducted in a H_2S corrosion experimental device based on the general NACE TM0284-2003 Standard [23]. A deoxygenating step was performed prior to the introduction of H_2S into the test solution. Thereafter, the flowmeter was used to maintain a positive pressure of H_2S gas. Test solution consisted of 5.0 wt.% sodium chloride dissolved in distilled water. The duration of

corrosion tests was 96 h. In addition, the temperatures of corrosion test were 25 °C, 40 °C, 60 °C and 90 °C, respectively.

2.3 Weight-loss tests

Weight loss tests were performed according to the ASTM G31 procedure [24]. Three specimens used for each tests were measured for good reproducibility. Prior to exposure to corrosion environments, the specimens were weighed by a digital balance (Sartorius BS110S) with a precision of 0.00001 g. The immersion time was 96 h. After corrosion tests, the specimens were removed from the corrosion device, then cleaned with distilled water and dried in air. The corrosion films on the steel surface were removed carefully by the chemical products-clean up method [25]. Finally, the specimens were weighted again to obtain the final weight. General corrosion rates (CR) were calculated based on the weight loss of the specimens.

2.4 Surface morphology observation and corrosion products analysis

After corrosion tests, surface morphology of corrosion films formed on the steel surface was examined by scanning electron microscopy (SEM) in an FEI Quanta 200F. The chemical compositions of the corrosion films were analyzed using a D/max-2500 V X-ray diffraction (XRD) with Cu Kα radiation generated at 40 kV and 200 mA, with a scanned range from 10 ° to 90 ° and a step size of 0.02 º.

2.5 Electrochemical measurement

A GAMRY 600 electrochemical test system was used for electrochemical measurements. A conventional three-electrode cell system was used with a sintered graphite rod as auxiliary electrode and a saturated calomel electrode (SCE) as reference electrode. In order to investigate the electrochemical characteristics of the corrosion films formed on the A350LF2 steel, the specimen subjected to the corrosion tests was used as the working electrode. The 5.0 wt.% potassium chloride solution was prepared with analytical reagents and deionized water. Electrochemical impedance spectroscopy (EIS) measurements were performed at open circuit potential (OCP) with the AC amplitude of a 10 mV (rms) sinusoidal perturbation and at the measurement frequency ranging from 100 kHz to 10 mHz.

3. RESULTS

3.1 Corrosion rates of carbon steel

With respect to the determination of corrosion rate, the most accurate and precise method is probably that of weight loss [26]. The corrosion rates of A350LF2 steel in 5 % NaCl solution saturated

with hydrogen sulfide at different temperatures is shown in figure 1. Error bars in this figure represent standard deviations of examined data.

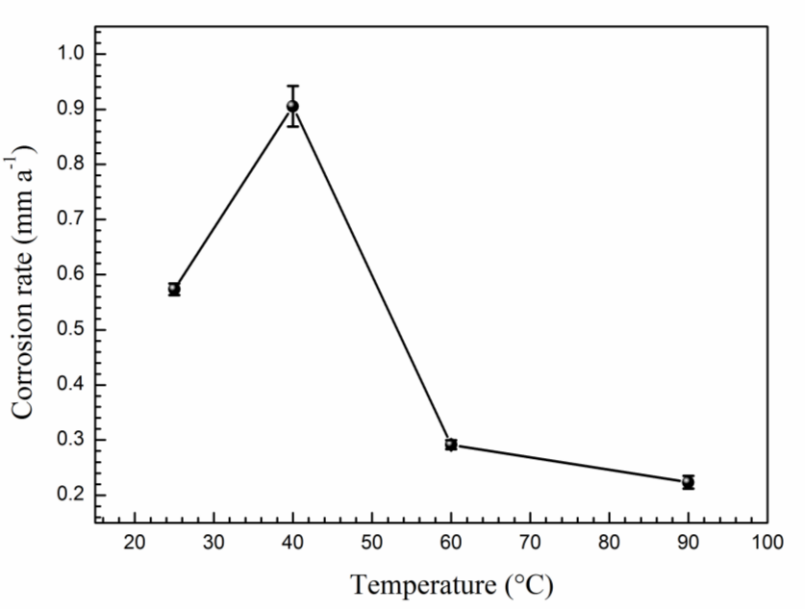

Figure 1. Plot of corrosion rates as a function of the temperature in 5 % NaCl solution saturated with hydrogen sulfide

It can be seen that the corrosion rate of A350LF2 steel increased significantly as temperature increased from 25 °C to 40 °C. With further increase of temperature, the corrosion rate decreased obviously. The corrosion rate could reach the maximum value (about 0.905 mm/a) at 40 °C, which was approximately 4-fold greater than that of A350LF2 steel at 90 °C (the minimum CR value: about 0.224 mm/a). The CR results indicated that A350LF2 steel was subjected to serious corrosion in 5 % NaCl solution saturated with hydrogen sulphide at different temperatures.

3.2 Morphology analysis of corrosion films

Figure 2 shows the SEM micrographs of corrosion films formed in 5 % NaCl solution saturated with H_2S at different temperatures for 96 h. It can be seen that corrosion film formed at 25 °C was uneven in the low resolution image (figure 2a), and some large cavities were observed in the corrosion films (figure 2a and b). Although some small cavities still existed in the corrosion film formed at 40 °C (figure 2c), the corrosion film at 40 °C became even and continuous compared with that at 25 °C (figure 2c and d). With further increase of temperature to 60 °C and 90 °C, the corrosion film became more even and continuous, as shown in the low resolution images (figure 2e and g). Moreover, no cavities could be found in the corrosion films. From the corresponding high resolution images (figure 2f and h), it can be seen that the grain of corrosion films at 60 °C and 90 °C exhibited a somewhat more fine and compact, indicative of good protection to the steel.

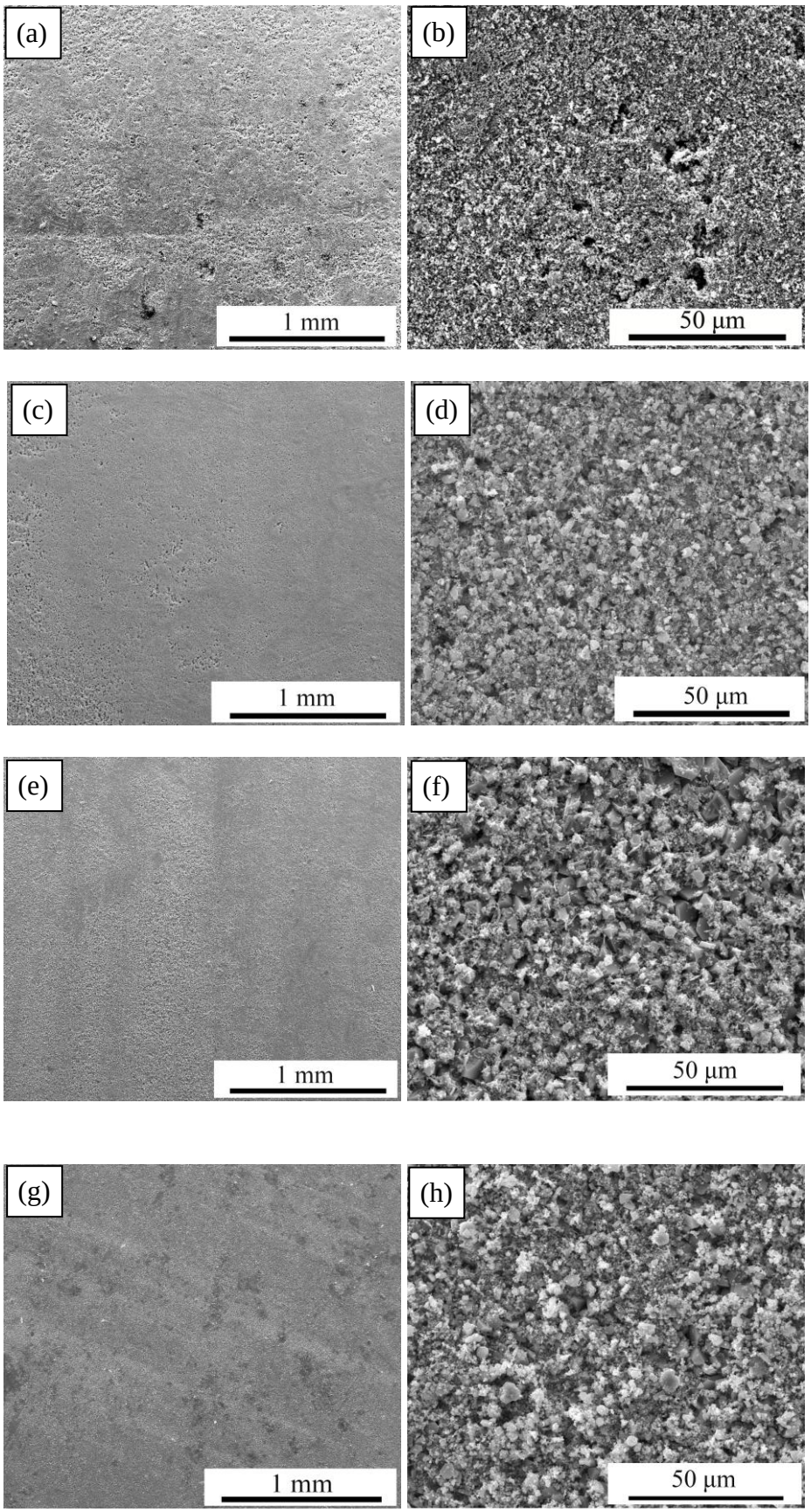

Figure 2. SEM micrographs of corrosion films formed in 5 % NaCl solution saturated with H_2S at different temperatures for 96 h. (a, b): 25 °C; (c, d): 40 °C; (e, f): 60 °C; (g, h): 90 °C.

3.3 Structural analysis of corrosion films

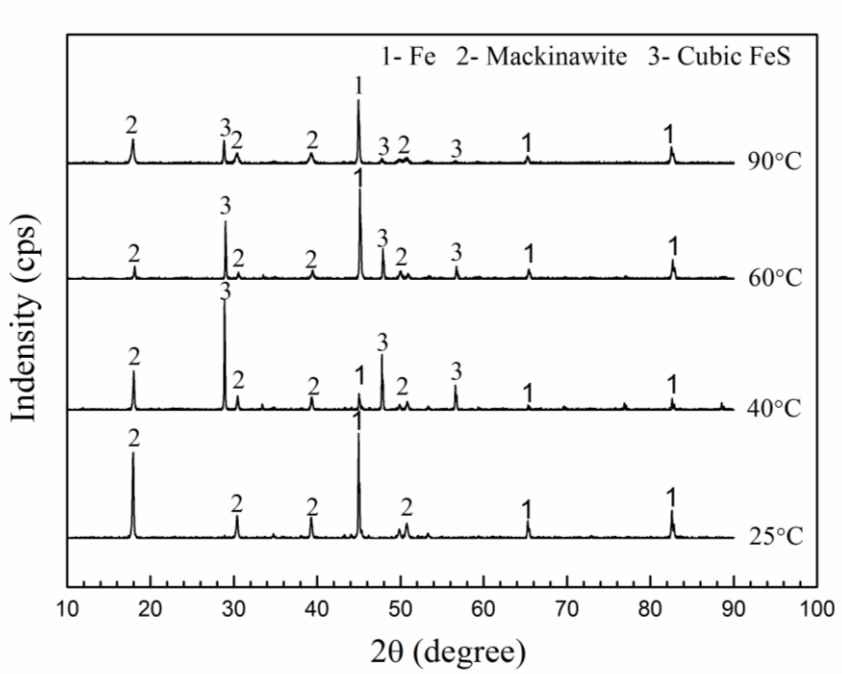

Figure 3. XRD analysis of corrosion films on carbon steel surface in 5 % NaCl solution saturated with H_2S at different temperatures for 96 h.

Figure 3 shows the XRD analysis of corrosion films on carbon steel surface in 5 % NaCl solution saturated with H_2S at different temperatures for 96 h. It was determined that the corrosion film formed at 25 °C just consisted of Mackinawite. Mackinawite, which has the chemical formula FeS_{1-x} (where x = 0.054-0.061) [27] is a prevalent type of iron sulphides [28-30] and usually forms as a precursor to other types of sulphides [31]. When temperature increased to 40 °C, an additional peak of cubic FeS was observed in the spectra on the basis of the peak of Mackinawite (figure 3). According to Shoesmith et al. [28] and Smith et al. [32], Mackinawite could transform to other stable forms of sulphides, for example cubic FeS. Shoesmith et al. [28] also proposed a conversion between machinawite and cubic FeS, which could be explained in terms of the close structural relationship between the phases. Moreover, cubic FeS would have a better protection against corrosion than Mackinawite [32]. With further increase of temperature to 60 and 90 °C, the corrosion films consisted of Mackinawite and cubic FeS, similar composition with that formed at 40 °C. It indicated that no corrosion film transformation occurred as temperature increased from 40 °C to 90 °C.

3.4 EIS measurements

Figure 4 depicts the behavior of EIS diagram of A350LF2 steel in 5% NaCl solution saturated with H_2S at different temperatures. As seen, all EIS diagrams exhibited a depressed semicircle with a capacitive arc. Additionally, the shape and size of Nyquist diagrams could be significantly affected by the temperature. The Nyqusit diagram corresponding to 25 °C possessed the smallest Z_{re} and Z_{im}

values compared to other temperatures. Furthermore, Z_{re} and Z_{im} values (or the diameter of capacitive semicircle) increased with an increase in temperature. This capacitive semicircle had something to do with the resistance in the corrosion process. According to the previous studies [33-35], the modifications of physicochemical properties of the corrosion films formed on the steel surface could be responsible for the diameter changes of capacitive semicircle, such as the density (figure 2), composition (figure 3) and electrical properties of corrosion films.

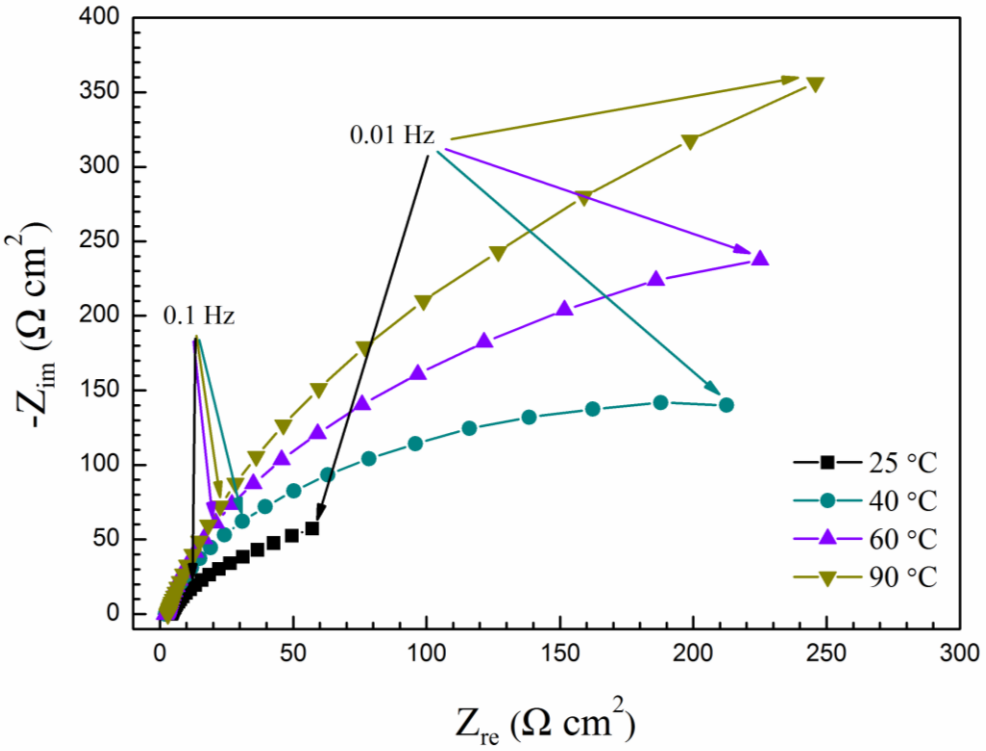

Figure 4. Nyquist diagram of A350LF2 steel in 5 % NaCl solution saturated with H_2S at different temperatures.

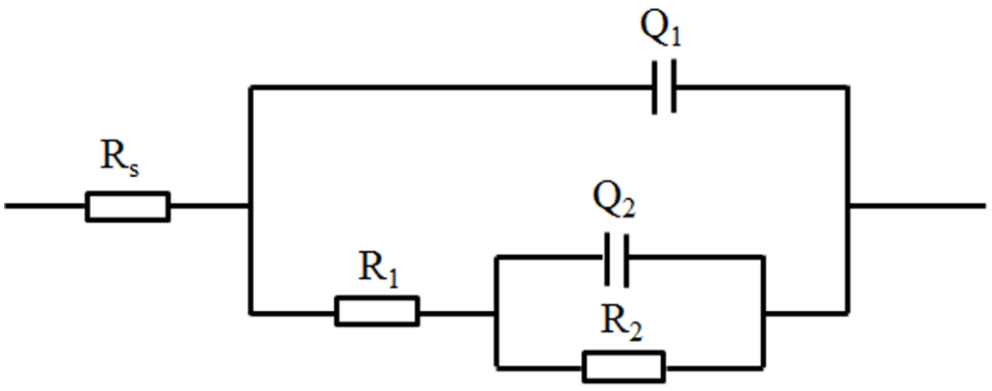

Figure 5. The electrochemical equivalent circuit for EIS fitting

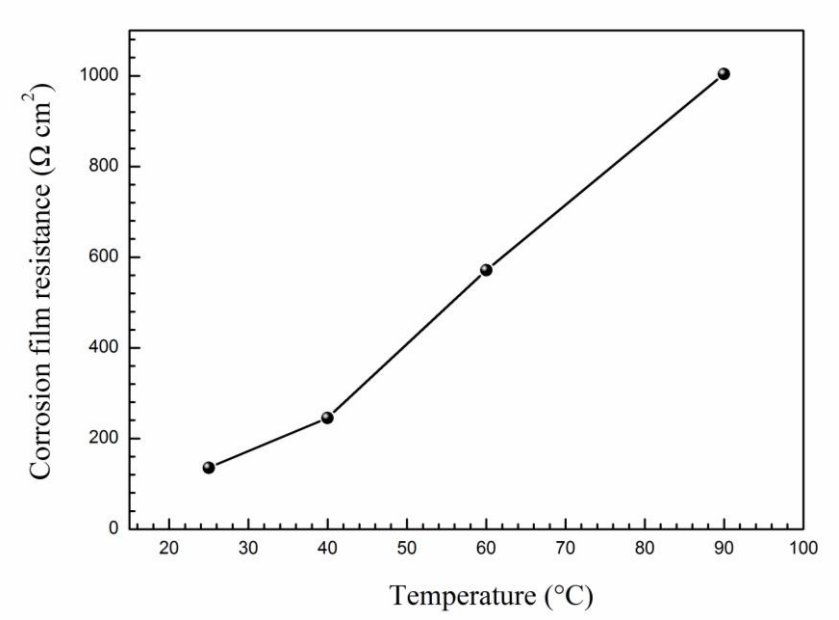

Figure 6. Evolution of corrosion film resistance with temperature obtained by fitting of EIS diagrams.

The proposed equivalent circuit used to fit the experimental data is shown in figure 5. In this equivalent circuit, R_s represents solution resistance; R_1 is the charge-transfer resistance in the steel/corrosion products interface; Q_1 is the double-layer capacitance between film and the solution; R_2 is corrosion film resistance and Q_2 is the constant phase element (CPE) representing double charge layer capacitance; Q_2-R_2 arrangement describes the diffusion of ions through the corrosion film on the steel surface [34]. The corrosion film resistance is an important parameter for the protectiveness against corrosion, which could indicate the diffusion resistance of ions (Fe^{2+}, HS^-, etc.) through the corrosion films. The evolution of corrosion film resistance with temperature is shown in figure 6. It can be seen that the corrosion film resistance increased with increasing temperature, which indicated that the diffusion resistance of ions through the corrosion films became enhanced. In addition, the slope of the line between 40 °C and 90 °C was obviously larger than that between 25 °C to 40 °C, which manifested that the corrosion film resistance increased rapidly when the temperature exceeded 40 °C. Based on the aforementioned results, it is concluded that the corrosion film could possess much better protectiveness to the steel as temperature increased.

4. DISCUSSION

In general, it is accepted that the corrosion process of carbon steel in aqueous medium with H_2S is carried out through the following mechanism [36-41]:

Anodic reaction: $Fe \rightarrow Fe^{2+} + 2e$

Dissociation reactions: $H_2S \rightarrow H^+ + HS^-$

$HS^- \rightarrow H^+ + S^{2-}$

Cathodic reaction: $2H^+ + 2e \rightarrow 2H\,(\text{atomic hydrogen}) \rightarrow H_2 \uparrow$

In this work, temperature is the sole parameter. Three main consequences should be considered as the temperature increased. 1) According to the Arrhenius equation, rate constant of corrosion reactions could increase with an increase in temperature. In addition, increasing the temperature can accelerate the diffusion of species involved in the electrochemical reactions. As a result, increasing temperature would increase the corrosion rate, resulting in promoting the corrosion of steel. 2) Temperature could affect the concentration of corrosion species (H_2S, H^+) that could affect the corrosion reaction. The solubility of hydrogen sulphide in NaCl solutions at different temperatures has been investigated by barrett et al. [42], as shown in figure 7.

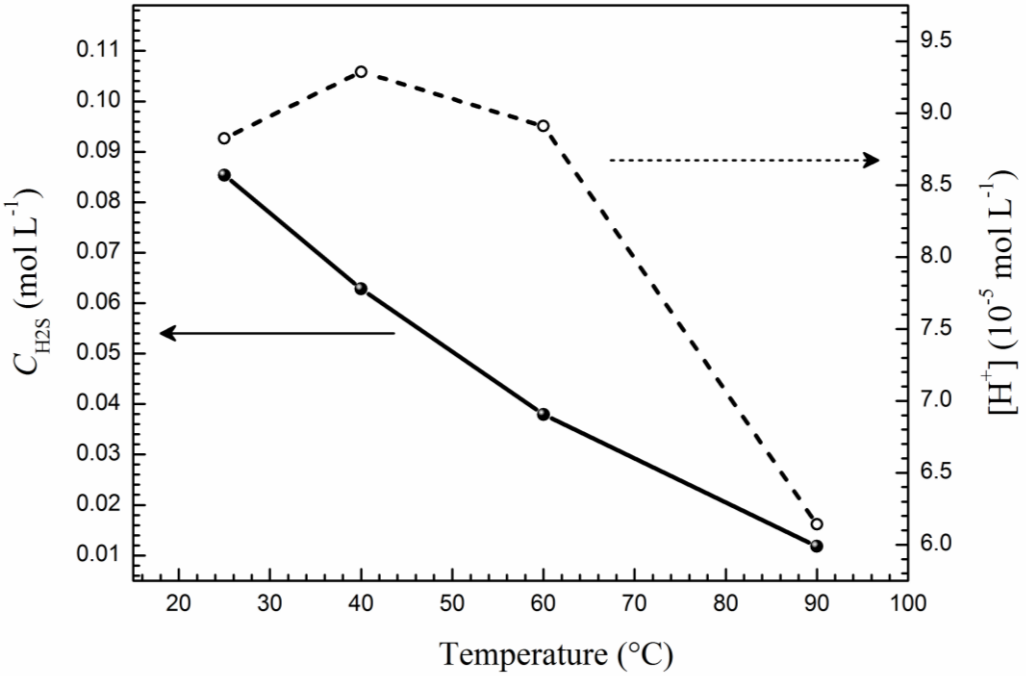

Figure 7. The variation of the concentrations of H_2S and H^+ with temperature

According to the dissociation reactions (mentioned above), the hydrogen ion concentration [H^+] is defined by

$$[H^+] = k_1 \times C_{H_2S} / [HS^-] \qquad (1)$$

Where k_1 is the first ionization constant of H_2S at different temperatures, C_{H2S} is the solubility of H_2S. The second ionization process could be ignored because the first ionization constant is much larger than the second ionization constant. Therefore, the equation (1) can be expressed as follows:

$$[H^+]^2 = k_1 \times C_{H_2S} \qquad (2)$$

In addition, it is known that the ionization constant varied with temperature. Based on the results of Ellis and Milestone [43], the first ionization constant of H_2S at different temperatures can be calculated by the following equation:

$$\log k_1 = -3760/T + 55.06 - 20\log T \quad (3)$$

According to equations (1) – (3), the concentrations of H^+ in 5% NaCl solution saturated with H_2S at different temperatures can be obtained. The variation of the concentrations of H_2S and H^+ with temperature is shown in figure 7. It can be seen that the concentrations of H_2S in NaCl solutions decreased significantly with increasing temperature. In addition, the concentrations of H^+ increased first and then decreased slightly when temperature increased from 25 °C and 60 °C. With further increase of temperature from 60 °C to 90 °C, the concentrations of H^+ decreased sharply. 3) Based on the results of figures. 2, 3, 4 and 6, it can be proved that temperature can affect the physicochemical properties of the corrosion films, such as the density, composition, etc.

According to the aforementioned three aspects induced by increasing temperature, the influence mechanism of temperature on the corrosion behavior of A350LF2 steel in wet H_2S environments was discussed in the following section. The variation curves of corrosion rate with temperature can be divided into three parts: part one (from 25 °C to 40 °C), part two (from 40 °C to 60 °C) and part three (from 60 °C to 90 °C). In the part one, the rate constant of corrosion reaction increased and the diffusion of corrosion species were accelerated when temperature increased from 25 °C to 40 °C. In addition, increasing temperature can also increase the concentrations of H^+ in this part (figure 7). As a result, the corrosion rate increased obviously in this part. Although corrosion film at 40 °C possessed better protectiveness than that at 25 °C (figures 2- 4), some small cavities still existed in the corrosion film formed at 40 °C (figure 2c). The protection of corrosion film on the steel was still insufficient compared to the attack of corrosion environments. As for the part two, the corrosion rate decreased sharply. However, the H^+ concentrations decreased slightly as temperature increased from 40 °C to 60 °C. On the other hand, the corrosion film became more even and continuous (figure 2e and f). Furthermore, the corrosion film resistance increased rapidly when the temperature exceeded 40 °C (figure 6). Thus, the diffusion resistance of ions (Fe^{2+}, H^+, etc.) through the corrosion films became enhanced. As a result, the content of corrosive ions at the interface between steel and corrosion films would decrease, resulting in decrease in the corrosion rate. It could be concluded that corrosion film plays a more dominant role in the decrease in corrosion rate than the H^+ concentration diminution. With further increase of temperature from 60 °C to 90 °C (part three), the H^+ concentration decreased obviously and the protectiveness of corrosion film further enhanced, which could be responsible for the decrease in corrosion rate in this section.

4. CONCLUSIONS

Temperature played a significant role in the corrosion rate of A350LF2 steel in hydrogen sulphide environment. The corrosion rate reached maximum value at 40 °C, then gradually decreased obviously with temperature. The increasing part of corrosion rate was mainly attributed to the diffusion enhancement of corrosive species and the increase in the H^+ concentration and the rate constant of corrosion reaction. High transport resistance of corrosion film and the decreasing H^+ concentration were responsible for the decrease in corrosion rate with further increase of temperature. In addition, corrosion films could have a more dominant role in the decrease in corrosion rate than the diminution of H^+ concentration.

ACKNOWLEDGEMENTS
This work was financially supported by the following funds: (1) Natural Science Foundation of China (No. 51171208 and No. 51271201); (2) National Science and Technology Key Specific Project: Life Management Technology of Nuclear Power Plant (Grant No. 2011ZX06004-002).

References

1. F. Hao, T.L. Guo, Y.M. Zhu, X.Y. Cai, H.Y. Zou and P.P. Li, *AAPG Bull.*, 92 (2008) 611.
2. T. Taira, K. Tsukada, Y. Kobayashi, H. Inagaki and T. Watanabe, *Corrosion*, 37 (1981) 5.
3. H. Pircher and G. Sussek, *Corros. Sci.*, 27 (1987) 1183.
4. G. Domizzi, G. Anteri and J. Ovejero-GarcÍa, *Corros. Sci.*, 43 (2001) 325.
5. L.W. Tsay, M.Y. Chi, H.R. Chen and C. Chen, *Mater. Sci. Eng., A*, 416 (2006) 155.
6. M.C. Zhao, M. Liu, A. Atrens, Y.Y. Shan and K. Yang, *Mater. Sci. Eng., A*, 478 (2008) 43.
7. S. Ramadan, L. Gaillet, C. Tessier and H. Idrissi, *Appl. Surf. Sci.*, 254 (2008) 2255.
8. J. Kittel, V. Smanio, M. Fregonese, L. Garnier and X. Lefebvre, *Corros. Sci.*, 52 (2010) 1386.
9. C.A. Zapffe and C.E. Sims, *Met. Alloys*, 12 (1940) 145.
10. R.A. Oriani and E.H. Josephic, *Acta Metall.*, 22 (1974) 1065.
11. A.R. Troiano, *Trans. ASM*, 52 (1960) 54.
12. C.D. Beachem, *Metall. Trans*, 3 (1972) 437.
13. H.K. Birnbaum and P. Sofronis, *Mater. Sci. Eng., A*, 176 (1994) 191.
14. P. Sofronis and H.K. Birnbaum, *J. Mech. Phys. Solids*, 43 (1995) 49.
15. H.Y. Ma, X.L. Cheng, S.H. Chen, C. Wang, J.P. Zhang and H.Q. Yang, *J. Electroanal. Chem.*, 451 (1998) 11.
16. H.Y. Ma, X.L. Cheng, G.Q. Li, S.H. Chen, Z.L. Quan, S.Y. Zhao and L. Niu, *Corros. Sci.*, 42 (2000) 1669.
17. M.A. Veloz and I. González, *Electrochim. Acta*, 48 (2002) 135.
18. H.H. Huang, J.T. Lee and W.T. Tsai, *Mater. Chem. Phys.*, 58 (1999) 177.
19. H.H. Huang, W.T. Tsai and J.T. Lee, *Electrochim. Acta*, 41 (1996) 1191.
20. S. Aezola and J. Genesca, *J. Solid State Electrochem.*, 8 (2005) 197.
21. J.W. Tang, Y.W. Shao, J.B. Guo, T. Zhang, G.Z. Meng and F.H. Wang, *Corros. Sci.*, 52 (2010) 2050.
22. J.W. Tang, Y.W. Shao, T. Zhang, G.Z. Meng and F.H. Wang, *Corros. Sci.*, 53 (2011) 1715.
23. NACE standard TM0284-2003, Evaluation of Pipeline and Pressure Vessel Steels for Resistance to Hydrogen-induced Cracking. NACE International.
24. ASTM Standard G31, Practice for Laboratory immersion corrosion testing of metals. ASTM International.
25. ISO 8407, Corrosion of metals and alloys-removal of corrosion products from corrosion test specimens. International Standardization Organization.
26. E. Poorqasemi, O. Abootalebi, M. Peikari and F. Haqdar, *Corros. Sci.*, 51 (2009) 1043.
27. J.S. Smith and J.D.A. Miller, *Br. Corros. J.*, 10 (1975) 136.
28. D.W. Shoesmith, P. Taylor, M.G. Bailey and D.G. Owen, *J. Electrochem. Soc.*, 127 (1980) 1007.
29. F.H. Meyer, O.L. Riggs, R.L. Mcglasson and J.D. Sudbury, *Corrosion*, 14 (1958) 69.
30. S. Arzola, J. Mendoza-Flores, R. Duran-Romero and J. Genesca, *Corrosion*, 62 (2006) 433.
31. W. Sun, S. Nešić, D. Young and Richard C. Woollam, *Ind. Eng. Chem. Res.*, 47 (2008) 1738.
32. S.N. Smith, M.W. Joosten, Proc. Conf. 'Corrosion/2006', Houston, TX, USA March 2006, NACE, paper 115.
33. A. Hernández-Espejel, M.A. Domínguez-Crespo, R. Cabrera-Sierra, C. Rodríguez-Meneses and E.M. Arce-Estrada, *Corros. Sci.*, 52 (2010) 2258.

34. E. Sosa, R. Cabrera-Sierra, M.E. Rinócn, M.T. Oropeza and I. González, *Electrochim. Acta,* 47 (2002) 1197.
35. V. Garcia-Arriaga, J. Alvarez-Ramirez, M. Amaya and E. Sosa, *Corros. Sci.*, 52 (2010) 2268.
36. W.K. Kim, S.U. Koh, B.Y. Yang and K.Y. Kim, *Corros. Sci.*, 50 (2008) 3336.
37. M.A. Lucio-Garcia, J.G. Gonzalez-Rodriguez and M. Casales, *Corros. Sci.,* 51 (2009) 2380.
38. S.Q. Zheng, Y.M. Qi, C.F. Chen and S.Y, Li, *Corros. Sci.*, 60 (2012) 59.
39. Y.M. Qi, H.Y. Luo, S.Q. Zheng, C.F. Chen and D.N. Wang, *Corros. Sci.,* 69 (2013) 164.
40. R. Cabrera-Sierra, E. Sosa, M.T. Oropeza and I. González, *Electrochim. Acta,* 47 (2002) 2149.
41. E. Sosa, R. Cabrera-Sierra, M.T. Oropeza, F. Hernández, N. Casillas, R. Tremont, C. Cabrera and I. González, *Electrochim. Acta,* 48 (2003) 1665.
42. T.J. Barrett, G.M. Anderson and J. Lugowski, *Geochim. Cosmochim. Acta*, 52 (1988) 807.
43. A.J. Ellis and N.B. Milestone, *Geochim. Cosmochim. Acta,* 31 (1967) 615.